



## Review

## Dual parallel mass spectrometry for lipid and vitamin D analysis

William Craig Byrdwell\*

USDA, ARS, Beltsville Human Nutrition Research Center, Food Composition and Methods Development Lab, 10300 Baltimore Ave., Beltsville, MD 20705, USA

## ARTICLE INFO

## Article history:

Available online 22 December 2009

## Keywords:

Lipids  
 Vitamin D  
 APCI-MS  
 ESI-MS  
 Mass spectrometry  
 Triacylglycerols  
 Phospholipids  
 Sphingomyelin  
 Milk  
 Orange juice

## ABSTRACT

There are numerous options for mass spectrometric analysis of lipids, including different types of ionization, and a wide variety of experiments using different scan modes that can be conducted. Atmospheric pressure chemical ionization (APCI) and electrospray ionization (ESI) provide complementary types of information that are both desirable. However, the duty cycle of the mass spectrometer places limits on the number of experiments that can be performed, and instruments usually employ only one type of ionization at a time. This work describes the approaches we have used that employ two mass spectrometers in parallel or in a column-switching configuration that allows multiple ionization modes and types of experiments to be conducted simultaneously during a single chromatographic run. These data demonstrate how use of two systems can reduce or eliminate the need for repeat injections and repetitive experiments. Approaches are described that employ two mass spectrometers connected in parallel as detectors for a single chromatographic system (LC1/MS2) or that employ two liquid chromatographs and two mass spectrometers in a column-switching arrangement (LC2/MS2). Examples of LC1/MS2 analyses of triacylglycerols (TAGs), sphingolipids, and vitamin D are given, as well as an example of an LC2/MS2 experiment that is used to perform analysis of both polar and non-polar lipids in a total lipid extract.

Published by Elsevier B.V.

## Contents

1. Introduction .....	3992
2. Materials and methods .....	3993
2.1. Materials .....	3993
2.2. Instrumentation .....	3993
2.2.1. LC1/MS2 Instrumentation for TAG .....	3993
2.2.2. LC1/MS2 Instrumentation for milk sphingomyelin .....	3993
2.2.3. LC1/MS2 instrumentation for vitamin D in orange juice .....	3993
2.2.4. LC2/MS2 Instrumentation .....	3994
3. Results and discussion .....	3994
3.1. LC1/MS2 of TAGs .....	3994
3.2. LC1/MS2 of bovine milk sphingomyelin .....	3996
3.3. LC1/MS2 of vitamin D <sub>3</sub> in orange juice .....	3999
3.4. LC2/MS2 of bovine brain total lipid extract .....	4000
4. Conclusion .....	4002
Acknowledgements .....	4003
References .....	4003

## 1. Introduction

Atmospheric pressure chemical ionization (APCI) mass spectrometry (MS) has become one of the primary methods of choice for analysis of vitamin D, triacylglycerols (TAGs) and other lipids

[1–5], because: (1) APCI is able to ionize large neutral molecules that are not amenable to other ionization methods, and (2) APCI produces gentle fragmentation, with large structurally informative fragments. APCI usually produces some protonated molecules in addition to abundant fragments, but not always. Electrospray ionization (ESI), on the other hand, yields almost exclusively protonated molecules or molecular adduct ions from lipids, with little or no fragmentation. Thus, these represent two ionization methods that produce different, and complementary, mass spectral informa-

\* Tel.: +1 301 504 9357; fax: +1 301 504 8314.

E-mail address: [C.Byrdwell@ARS.USDA.gov](mailto:C.Byrdwell@ARS.USDA.gov).

tion, both of which are useful and desirable. A thorough compilation of literature reports of APCI-MS for lipid analysis can be found on the Lipid Library APCI-MS literature survey page [6], while a similarly thorough list of literature reports describing ESI-MS for lipid analysis is found at the Lipid Library ESI-MS literature survey page [7].

Most mass spectrometers allow only one ionization mode to be performed at a time. Usually, the ionization source must be changed and separate experiments conducted to obtain data from these two complementary ionization modes. To overcome this limitation, we have previously demonstrated several examples of the use of two mass spectrometers that employ different ionization modes that are both connected as detectors on a single chromatographic system, referred to as an LC1/MS2 configuration. In this report, examples of the analysis of triacylglycerols and of sphingomyelin species using both APCI-MS and ESI-MS simultaneously in parallel, to take advantage of these two powerful ionization modes are given.

Another important reason that two mass spectrometers employed in parallel can be a valuable tool is that often two or more types of scan modes or scan experiments must be conducted. Since any mass spectrometer has limitations placed on it by scan speed, processing speed, between-scan switching and settling times, and other factors, it is often not optimal or simply not possible to run all of the desired experiments during a single run. For instance, selected ion monitoring (SIM) has been used for vitamin D analysis, but if chromatographic resolution is not perfect, there may be overlapping species that are not evident when monitoring only selected ions. Therefore, it is desirable to obtain full-scan or MS/MS data in addition to SIM data to confirm the purity of chromatographic peaks and to identify any interfering species when present. Two examples are presented here in which quantification is conducted using SIM APCI-MS, while full-scan APCI-MS data are simultaneously acquired in parallel for qualitative identification.

Another problem that often arises is due to the complexity of lipid mixtures in biological systems. Typical extraction procedures, such as the Folch extract [8], or that of Bligh and Dyer [9], produce complex mixtures of both polar lipids, such as phospholipids, and non-polar lipids, such as TAGs. Phospholipids are typically analyzed using normal-phase (NP) HPLC for a separation by classes, while triacylglycerols are usually analyzed using reversed-phase (RP) HPLC. Therefore, either polar or non-polar lipids are typically analyzed to the exclusion of the other. However, multi-dimensional chromatography has become more common and popular in recent years [10–15]. This approach is especially applicable to the growing field of lipidomics [16–18], in which knowledge of all molecular species of all lipid classes is sought. Although the non-chromatographic approach of 'shotgun lipidomics' pioneered by Han and Gross [19,20] has been shown to be very effective for a variety of samples, and is becoming more widespread, it is often preferable to take advantage of the additional information provided by a chromatographic separation in combination with mass spectrometry. Separation of classes prior to analysis allows the source and fragmentation parameters and the duty cycle of the mass spectrometer to be optimized for each class of lipid, and multiple injections are not required. This report describes a dual chromatography (NP-HPLC and RP-HPLC) column-switching arrangement with simultaneous detection by two mass spectrometers, referred to as an LC2/MS2 approach, for analysis of polar and non-polar lipids in a cellular extract.

## 2. Materials and methods

The dual parallel mass spectrometer arrangement used in our lab required no special or fabricated equipment. Simple tees were

used to split the flow between the two mass spectrometers, with the relative flow rates dictated by the lengths and internal diameters of the tubing used. Other auxiliary detectors, such as a UV detector or an evaporative light scattering detector (ELSD), were also usually used. Specific tubing connections and different combinations of detectors are described in the publications cited below. Nomenclature for phospholipids is taken from the updated classification scheme for lipids [21].

### 2.1. Materials

Commercially available canola oil was purchased from a local market. Bovine milk sphingomyelin (BMS) and bovine brain whole lipid extract (BBE) were purchased from Avanti Polar Lipids (Alabaster, AL, USA). All solvents, except water, were purchased from either Aldrich Chemical Co. (St. Louis, MO) or Fisher Scientific (Fair Lawn, NJ). HPLC grade solvents were purchased and were used without further purification. Water was obtained from a Millipore (Waters, Inc., Milford, MA) 'Milli-Q Academic' deionized water filtration system and was used without further purification. Orange juice samples analyzed for vitamin D were collected from stores across the United States between April and June of 2007 as part of the National Food and Nutrient Analysis Program (NFNAP) [22], and were sent to the Virginia Tech Food Analysis Laboratory Control Center (FALCC) for processing. Orange juice samples were extracted using the ether/petroleum ether extraction procedure from AOAC 992.26 [23].

### 2.2. Instrumentation

#### 2.2.1. LC1/MS2 Instrumentation for TAG

For TAG analysis using the LC1/MS2 approach, we employed an acetonitrile/dichloromethane solvent system. The typical solvent gradient used for the TAG analysis is as described in our first report of dual parallel mass spectrometry [24]. A Finnigan MAT TSQ 700 (Finnigan MAT, now Thermo Fisher Scientific Inc., San Jose, CA, USA) was used for acquisition of APCI-MS data while an LCQ Deca (Finnigan MAT, now Thermo Fisher Scientific Inc., San Jose, CA) ion trap mass spectrometer was used for acquisition of ESI-MS data.

#### 2.2.2. LC1/MS2 Instrumentation for milk sphingomyelin

A normal-phase HPLC separation on amine columns was carried out using two adsorbosphere NH<sub>2</sub> columns (Alltech Associates, Deerfield, IL, USA), 25.0 cm × 4.6 mm, 5 μm particle size, in series. A Varex MKIII evaporative light scattering detector (Varex, Burtonsville, MD, USA) was attached to the mass spectrometer as an auxiliary detector. The gradient program has been previously described [25]. The dual parallel mass spectrometers used for sphingomyelin analysis were the same as those described above for TAG analysis. Positive-ion full-scan APCI-MS was performed on the TSQ 700 mass spectrometer. Positive- and negative-ion ESI-MS were performed on the LCQ Deca ion trap mass spectrometer, with 20 mM ammonium formate solution in H<sub>2</sub>O/ACN (1:4) added as a sheath liquid at a rate of 20 μL/min.

#### 2.2.3. LC1/MS2 instrumentation for vitamin D in orange juice

Vitamin D analysis required two chromatographic separations, a preparative NP-HPLC separation in which vitamin D<sub>2</sub> and D<sub>3</sub> eluted together and were diverted to a fraction collector, and a RP-HPLC analytical separation. Vitamin D<sub>2</sub> and D<sub>3</sub> were separated on the RP-HPLC system, and vitamin D<sub>3</sub> was quantified based on 1.0 mL of 0.5 μg/mL vitamin D<sub>2</sub> added as an internal standard to each ~30 mL sample prior to extraction. The solvent program and other conditions were recently described [26]. A TSQ 7000 mass spectrometer (Finnigan MAT, now Thermo Fisher Scientific Inc., San Jose, CA, USA) was operated in Q3 SIM mode, using the protonated molecule

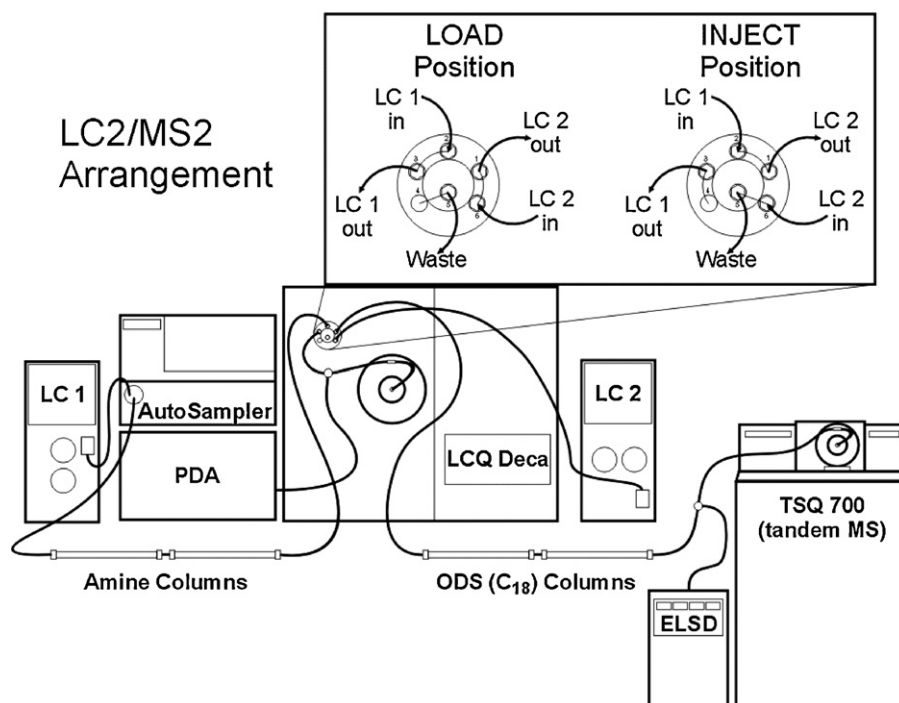


Fig. 1. Arrangement of instruments for dual liquid chromatography/dual mass spectrometry (LC2/MS2) experiments.

$[M+H]^+$ , at  $m/z$  397.3 and the dehydrated protonated molecule,  $[M+H-H_2O]^+$ , ion at  $m/z$  379.3 for the vitamin D<sub>2</sub> internal standard, and the  $[M+H]^+$  at  $m/z$  385.3 and the  $[M+H-H_2O]^+$  ion at  $m/z$  367.3 for vitamin D<sub>3</sub>. APCI on the LCQ Deca XP was performed with a combination APCI/APPI source from Syagen, Inc. (Tustin, CA), in APCI-only mode, using the same parameters as used on the TSQ7000 instrument.

#### 2.2.4. LC2/MS2 Instrumentation

For LC2/MS2 experiments, a normal-phase liquid chromatographic system was attached to an ion trap mass spectrometer, while a reversed-phase LC system was attached to a tandem mass spectrometer. The gradient program has been previously described [10]. Less than optimal chromatographic conditions were used for the RP-HPLC separation, compared to the conventional ACN/DCM gradient, to make it more compatible with the NP-HPLC solvent system. The interconnections between the two liquid chromatographic systems, the two auxiliary detectors (PDA and ELSD), and the two mass spectrometers (the ion trap mass spectrometer and the tandem mass spectrometer) are shown in Fig. 1.

### 3. Results and discussion

#### 3.1. LC1/MS2 of TAGs

Fig. 2 shows the RP-HPLC-APCI-MS separation of canola oil TAGs. Fig. 2A and B depicts the APCI-MS data showing alternating MS and MS/MS scans, and filtered full scans, respectively. Mass spectra were selected that demonstrate two points: (1) the difference between the fragmentation of polyunsaturated TAG vs. TAG with few sites of unsaturation; (2) the APCI-MS spectra of late-eluting TAG containing long-chain fatty acids (FA), C20–C24, present at low levels, for comparison to ESI-MS (Fig. 3). As we described in our first report of RP-HPLC-APCI-MS of TAGs [27], polyunsaturated TAGs give a protonated molecule base peak, such as that for dilinoleoyl, oleoyl triacylglycerol (LLO) in Fig. 2D, whereas TAGs with few sites of unsaturation give a diacylglycerol-like fragment ion,  $[DAG]^+$ , as the base peak. The  $[DAG]^+$  fragment ions at  $m/z$  599.4 and  $m/z$  601.4

identify the  $[LL]^+$  and  $[OL]^+$  peaks, respectively. However, the distribution of the unsaturation among the FAs also affects the ratio of the fragments. Dioleoyl, linoleoyl triacylglycerol (OOLn) is isobaric with LLO and gave the same protonated molecule mass at  $m/z$  881.6, but the base peak was  $m/z$  599.4 in Fig. 2E, instead of the  $[M+H]^+$ . The combination of the  $m/z$  599.4, representing  $[OLn]^+$ , combined with  $m/z$  603.4, representing  $[OO]^+$ , allowed the structure of the TAG to be characterized. When the unsaturation was more evenly distributed (i.e. LLO), a protonated molecule was the base peak, whereas when the unsaturation was concentrated in one FA (i.e. OOLn), a  $[DAG]^+$  fragment was the base peak.

The APCI-MS/MS spectrum of OOLn is shown in Fig. 2F, and exhibited mostly fragments arising from the oleoyl FA, specifically the  $[RCOO+58]^+$  peak at  $m/z$  339 and the acylium ion,  $[RCO]^+$  at  $m/z$  265, as well as other fragments.

The remaining mass spectra in Fig. 2 demonstrate detection of overlapping TAGs present at low levels. Fig. 2G–I shows mass spectra at the beginning, middle and end of a small peak eluted from ~75.5 to 76.3 min. TAGs with few sites of unsaturation eluted in this retention time range. The primary TAG at that time was dioleoyl, stearoyl triacylglycerol (OOS), which gave  $[DAG]^+$  peaks at  $m/z$  603.4 ( $[OO]^+$ ) and  $m/z$  605.4 ( $[OS]^+$ ) in Fig. 2H.  $[DAG]^+$  fragments from TAGs having the same calculated mass of 887.8 amu allowed at least two other isobaric molecular species to be identified. Fig. 2G shows the  $m/z$  577.4 and  $m/z$  631.4  $[DAG]^+$  fragments representing  $[PO]^+$  (16:0,18:1) and  $[OG]^+$  (18:1,20:1), respectively, that, along with the protonated molecule at  $m/z$  887.7, identified the TAG palmitoyl, oleoyl, gadoleoyl triacylglycerol (POG). The  $m/z$  605.3 representing  $[PG]^+$  was isobaric with  $[OS]^+$  from the overlapping OOS, so was not unique. Similarly, Fig. 2I shows fragments at  $m/z$  575.4,  $m/z$  607.4 and  $m/z$  631.4 that identified the  $[PL]^+$ ,  $[PA]^+$  and  $[LA]^+$  peaks from PLA that was also isobaric and overlapped OOS.

One more example to highlight the difference between APCI-MS and ESI-MS/MS is given. Fig. 2J–L shows the APCI-MS mass spectra at the beginning, middle and end of a small chromatographic peak eluted from ~81 to 82 min. The primary TAG at that time was dioleoyl, behenyl triacylglycerol (OOB), which gave the mass

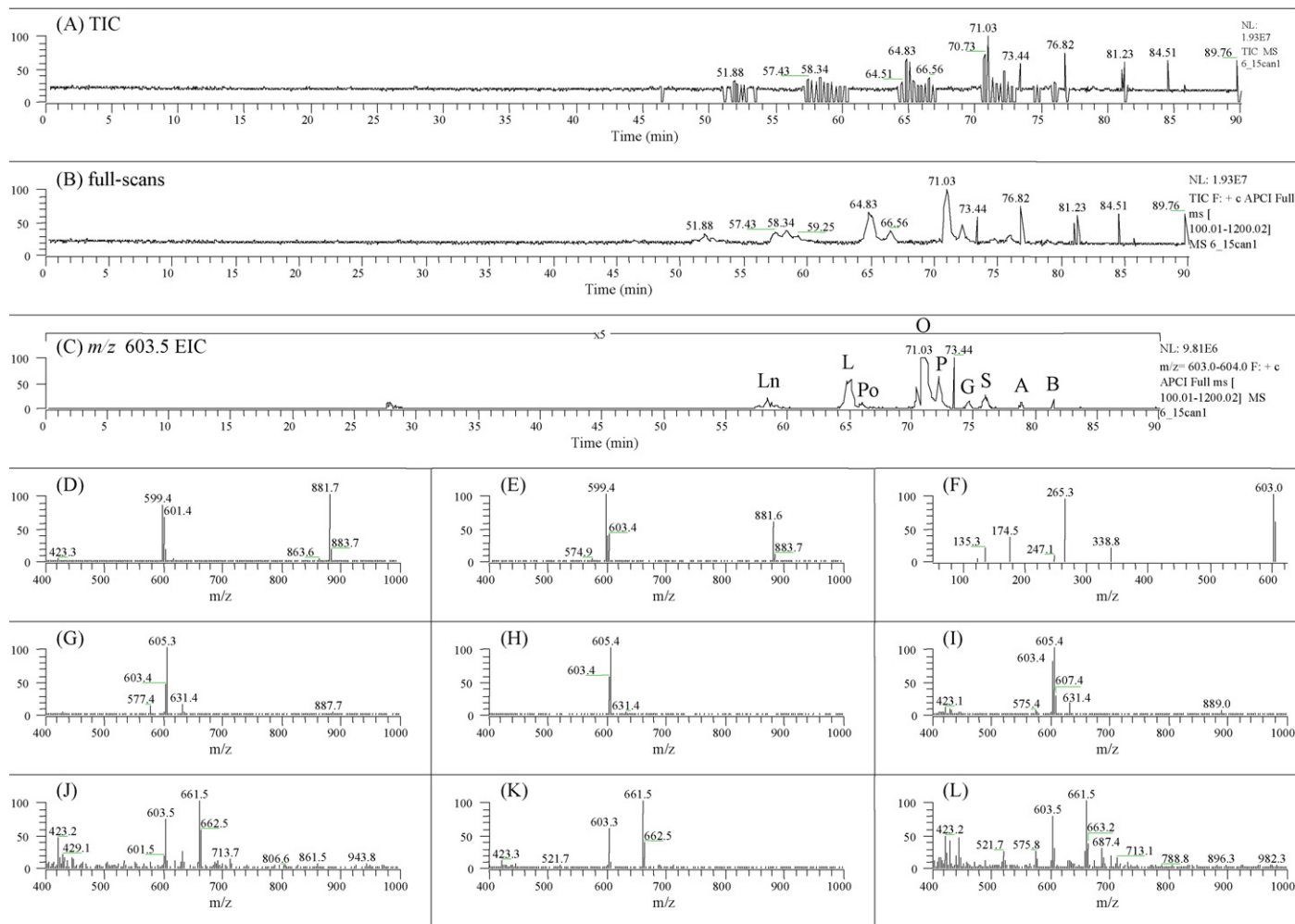


**Fig. 2.** Atmospheric pressure chemical ionization (APCI) mass spectrometry (MS) of canola oil separated by RP-HPLC. (A) Total ion current chromatogram (TIC); (B) TIC filtered to show full scans; (C) extracted ion chromatogram (EIC) of  $m/z$  603.5 =  $[OO]^+$ ; (D) average mass spectrum at  $\sim 57.5$  min; (E) spectrum at  $\sim 58.3$  min; (F) MS/MS spectrum of  $m/z$  603.5 at  $\sim 58.5$  min; (G) mass spectrum at  $\sim 75.6$  min; (H) spectrum at  $\sim 76.1$  min; (I) spectrum at  $\sim 76.4$  min; (J) spectrum at  $\sim 81.2$  min; (K) spectrum at  $\sim 81.5$  min; (L) spectrum at  $\sim 81.8$  min. ELSD not shown.

spectrum in Fig. 2K. The  $[OO]^+$  fragment at  $m/z$  603.3 and  $[OB]^+$  at  $m/z$  661.5 made this TAG straightforward to identify. The isobaric TAGs palmitoyl, oleoyl, nervonyl triacylglycerol (PON) and palmitoyl, linoleoyl, lignoceroyl triacylglycerol (PLLg) were more difficult to identify using this detector. Fig. 2] shows small but visible (unlabeled) peaks at  $m/z$  577.8 and  $m/z$  687.8 representing  $[PO]^+$  and  $[ON]^+$ , respectively, with  $[PN]^+$  isobaric and indistinguishable from  $[OB]^+$  at  $m/z$  661.5. Much more definitive fragments from this TAG are seen in Fig. 3, discussed below. Fig. 2L shows fragments at  $m/z$  575.8,  $m/z$  663.2, and  $m/z$  687.4 that correspond to  $[PL]^+$ ,  $[PLg]^+$ , and  $[LLg]^+$ , respectively, that arose from palmitoyl, linoleoyl, lignoceroyl triacylglycerol (PLLg), in the presence of the peaks from OOB mentioned above. However, this TAG was present in such a low amount that the signal-to-noise ratio was poorer.

An important benefit of the in-source fragmentation that occurs during APCI to produce diacylglycerol-like fragment ions is that extracted ion chromatograms (EICs) produced by extracting out the fragment ions for each  $[DAG]^+$  provide valuable chromatographic information to supplement the mass spectral data. In any given EIC, such as the one shown in Fig. 2C, a peak occurs for every TAG that contains the  $[DAG]^+$  fragment. Furthermore, the elution pattern shows the elution of TAG in order of equivalent carbon number (ECN), which is the number of carbon atoms in the FA chains (the acyl carbon number, ACN) minus two times the number of double

bonds,  $ECN = ACN - 2DB$ . Within an ECN group (e.g. 18:2, 16:1, 14:0, all ECN 14), the FA elute by degree of unsaturation—most to least. Thus, the peaks in Fig. 2C can be seen to obey the elution pattern Ln, L, Po, M, O, P, G, S, A, B, for the dioleoyl  $[DAG]^+$ ,  $[OO]^+$ , combined with linolenic, linoleic, palmitoleic, myristic (when present), oleic, palmitic, gadoleic, stearic, arachidic, and behenic acid containing TAG, respectively. Such EICs are valuable for locating low-level TAG for which the mass spectrum alone is not definitive, such as OOB seen in Fig. 2K.

ESI-MS,  $-MS/MS$  and  $-MS^3$  mass spectral data, shown in Fig. 3, were obtained in parallel with the APCI-MS data in Fig. 2. Since TAGs are large neutral molecules that are not amenable to electrospray ionization, ammonium formate was added as a sheath liquid (plumbed to the ESI source) to promote formation of ammonium adducts. As Fig. 3A shows, many more chromatographic peaks were evident from ESI-MS of ammonium adducts than were seen in the APCI-MS total ion current chromatogram (TIC) in Fig. 2A. Not only was ESI-MS very sensitive for TAG, but also polyunsaturated TAG gave more signal than saturated and moderately unsaturated TAG, as shown by the larger size of the early-eluting peaks in Fig. 3A. Nevertheless, ESI-MS was still very sensitive for TAG with few sites of unsaturation, as seen from the large number of late-eluting peaks. For direct comparison, mass spectra are shown that were averaged over the same peaks as those shown in Fig. 2D–L. The first impor-

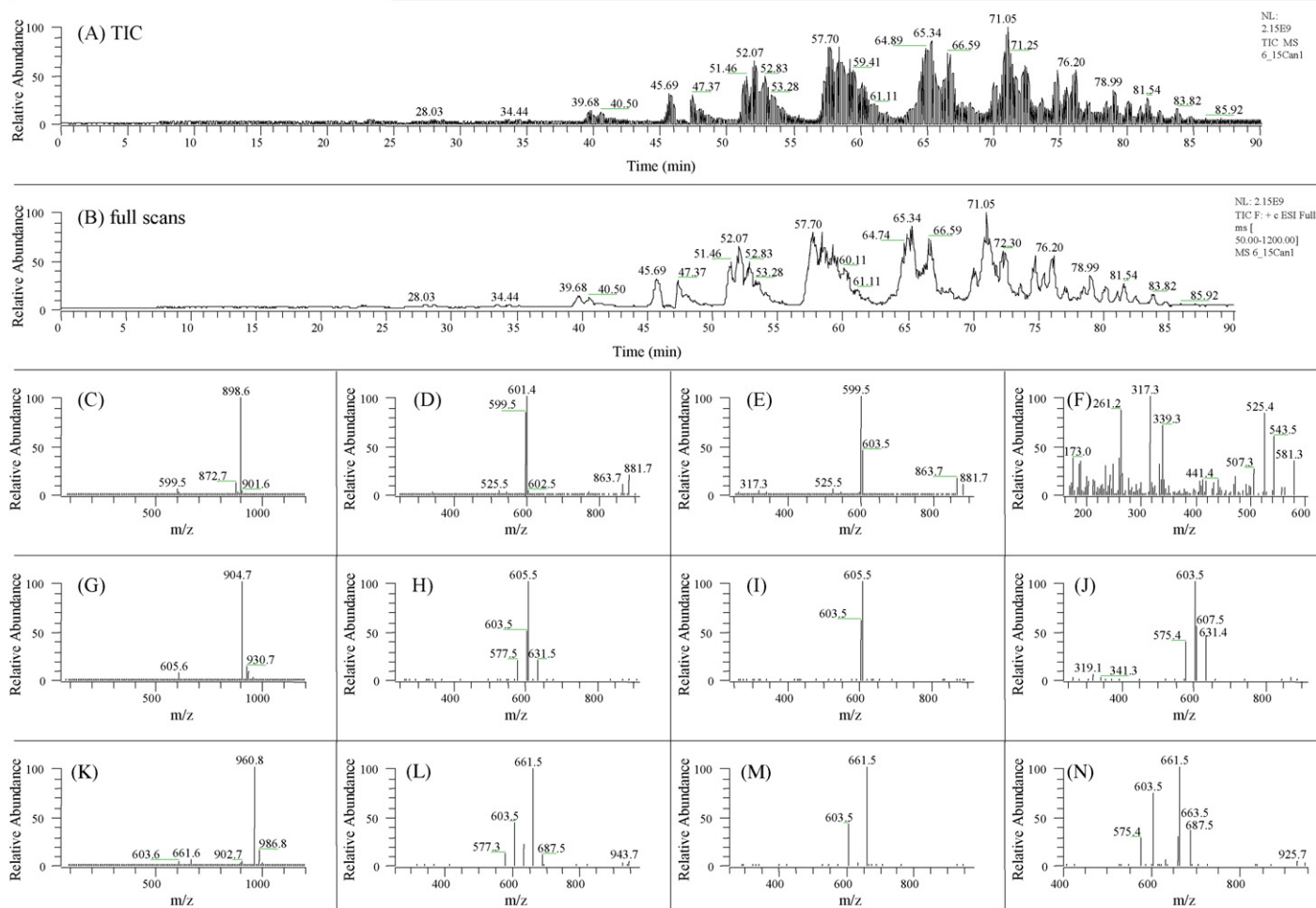


**Fig. 3.** Electrospray ionization (ESI) MS, MS/MS and MS<sup>3</sup> in parallel with APCI-MS in Fig. 2. (A) TIC; (B) TIC filtered to show full scans; (C) average mass spectrum from 57 to 60 min; (D) MS/MS spectrum of  $m/z$  898.7 at ~57.5 min; (E) MS/MS spectrum of  $m/z$  898.7 at ~59.2 min; (F) MS/MS/MS mass spectrum of  $m/z$  898.7 →  $m/z$  599.5 at ~59.2 min; (G) full-scan spectrum at ~76.1 min; (H) MS/MS spectrum of  $m/z$  904.7 at ~75.7 min; (I) MS/MS spectrum of  $m/z$  904.7 at ~76.1 min; (J) MS/MS spectrum of  $m/z$  904.7 at ~76.6 min; (K) full-scan spectrum at ~81.6 min; (L) MS/MS spectrum of  $m/z$  960.8 at ~81.3 min; (M) MS/MS spectrum of  $m/z$  960.8 at ~81.5 min; (N) MS/MS spectrum of  $m/z$  960.8 at ~81.9 min.

tant difference between the APCI-MS and ESI-MS spectra is that ESI-MS spectra exhibited ammonium adducts as base peaks, with only small abundances of [DAG]<sup>+</sup>. Because of this, EIC such as that shown in Fig. 2C are often not available for facile characterization of the elution pattern of TAG described above. However, the large abundances of ammonium adducts made them ideal as precursors for MS/MS. The ESI-MS spectrum shown in Fig. 3C is across the same LLO peak described in Fig. 2D. The base peak of  $m/z$  898.6 represents the ammonium adduct, [M+NH<sub>4</sub>]<sup>+</sup>, of LLO. ESI-MS/MS spectra of this precursor ion at two different times are seen in Fig. 3D and E. These spectra exhibit the same protonated molecule, [M+H]<sup>+</sup>, at  $m/z$  881.7 to provide confirmation of the molecular weight deduced from the ammonium adduct. The [DAG]<sup>+</sup> fragments are the same as those shown in Fig. 2D and E, in similar abundances, allowing differentiation of LLO (Figs. 2D and 3D) from OOLn (Figs. 2E and 3E). Because of the large abundance of the original precursor ion, an excellent average ESI-MS<sup>3</sup> spectrum, Fig. 3F, was obtained from the  $m/z$  599.5 product ion in the spectrum shown in Fig. 3E.

The ESI-MS spectrum in Fig. 3G corresponds to the peak from 75.5 to 76.7 min, and encompasses the three TAG shown in Fig. 2G–I. The ESI-MS/MS spectra of the  $m/z$  904.7 precursor ion are shown in Fig. 3H, I, and J, and show a striking similarity to the corresponding APCI-MS spectra in Fig. 2G–I. The small [DAG]<sup>+</sup> peaks are more readily apparent in the ESI-MS/MS spectrum, such as the  $m/z$  575.4 and  $m/z$  631.4 in Fig. 3J that allow PLA, present in a small amount,

to be identified. This benefit is even more evident in Fig. 3L–N. The precursor ammonium adduct at  $m/z$  960.8 in Fig. 3K is mostly OOB, as seen by the small abundances of [DAG]<sup>+</sup> in the full-scan spectrum, and further seen in Fig. 3M. But ESI-MS/MS at the beginning and the tail of the peak, Fig. 3L and N, respectively, clearly show the [DAG]<sup>+</sup> fragments that allowed PON and PLLg, discussed above to be identified. The signal-to-noise ratio in the product ion spectra is better than in the APCI-MS full-scan spectra since the first stage of the ion trap ESI-MS/MS filtered out all other chromatographically overlapped non-isobaric species. Because of this precursor → product relationship, the [DAG]<sup>+</sup> fragments in the ESI-MS/MS spectra are more definitive than the same [DAG]<sup>+</sup> fragments in the APCI-MS full-scan spectra, since the latter relied on comparison of multiple EICs, such as that in Fig. 2C, to conclusively identify co-eluting species. Thus, while the EICs from APCI-MS made locating TAG easier, especially at low levels, the ESI-MS/MS spectra were more definitive for their unambiguous identification. Therefore, both APCI-MS and ESI-MS and MS/MS are valuable and have complementary benefits, making a dual parallel mass spectrometer arrangement worthwhile for TAG analysis.

### 3.2. LC1/MS2 of bovine milk sphingomyelin

We have recently applied a dual parallel mass spectrometer approach to identification of sphingomyelin (SM) from a vari-

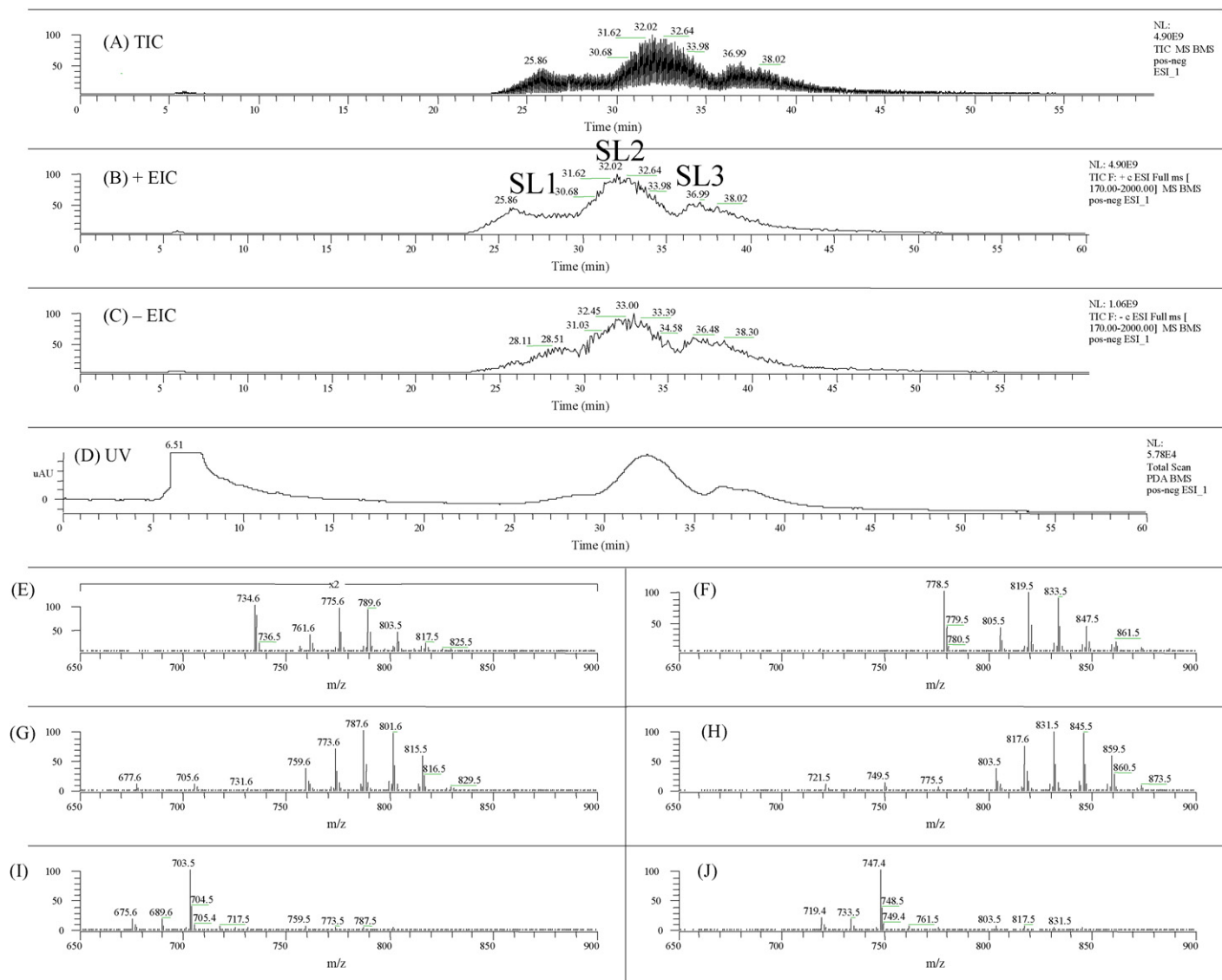


**Fig. 4.** ESI-MS alternating positive- and negative-ion modes for bovine milk sphingomyelin analysis. (A) TIC; (B) TIC filtered to show positive-ion scans; (C) TIC filtered to show negative-ion scans; (D) UV total scan chromatogram; (E) average positive-ion mass spectrum across SL1, 26–29 min; (F) average negative-ion spectrum across SL1; (G) average positive-ion spectrum across SL2, 29.75–35.5 min; (H) average negative-ion spectrum across SL2; (I) average positive-ion spectrum across SL3, 35.6–40 min; (J) average negative-ion spectrum across SL3.

ety of sources [25,28]. In the same way that APCI-MS produced fragments from TAGs, so, too, does it produce fragments, with minimal protonated molecules from choline-containing sphingolipids. This allows direct identification of the ceramide-like fragment formed by loss of the choline head group. APCI-MS is especially valuable because choline-containing phospholipids, including sphingomyelin and glycerophosphocholine, do not typically produce these fragments from ESI-MS/MS. Instead ESI-MS/MS usually produces primarily the  $m/z$  184.2 phosphocholine fragment, which provides no structural information about the ceramide backbone. Furthermore, since ceramide fragments are not formed, they are not available for further fragmentation to allow additional characterization of the long-chain base and the fatty amide by ESI-MS<sup>3</sup>.

Fig. 4 shows the ESI-MS chromatograms and mass spectra of milk sphingomyelin. The TIC in Fig. 4A shows all spectra, with alternating positive- and negative-ion modes. The positive-scan filtered EIC is shown in Fig. 4B, while the negative-scan filtered EIC is seen in Fig. 4C. These can be compared to the conventional UV total scan spectrum in Fig. 4D. ESI-MS spectra are shown in

Fig. 4E–J, and since no fragments were formed in the source, only the range  $m/z$  650–900 is shown. The positive-ion spectra in Fig. 4E, G and I exhibit only protonated molecules, which readily allow the molecular weights of the sphingomyelin species across sphingolipid peaks SL1, SL2, and SL3 to be identified. The key point in these spectra is that for every peak in SL2 (Fig. 4G) there is a peak in SL1 (Fig. 4E) at two mass units higher, and for every peak in SL3 (e.g.  $m/z$  703.5,  $m/z$  675.6, Fig. 4I), there is a peak in SL2 at two mass units higher (e.g.  $m/z$  705.5,  $m/z$  677.6). This difference of 2 mass units has led to a great deal of confusion in the past, and data such as these in Figs. 4 and 5 have shown that chromatographic resolution of sphingomyelin is crucial to proper identification of all molecular species. This is because we have shown, and Figs. 4 and 5 exemplify, the fact that most sphingomyelin (e.g. bovine brain and bovine milk and to a much lesser extent chicken egg yolk) actually contains a substantial proportion of dihydrosphingomyelin (DSM), which differs from sphingomyelin by 2 mass units, caused by the absence of the 4,5-*trans* double bond. This means that any DSM molecular species that has one double bond in the fatty amide chain has the same mass as a SM species with the same carbon chain length but no double bond.

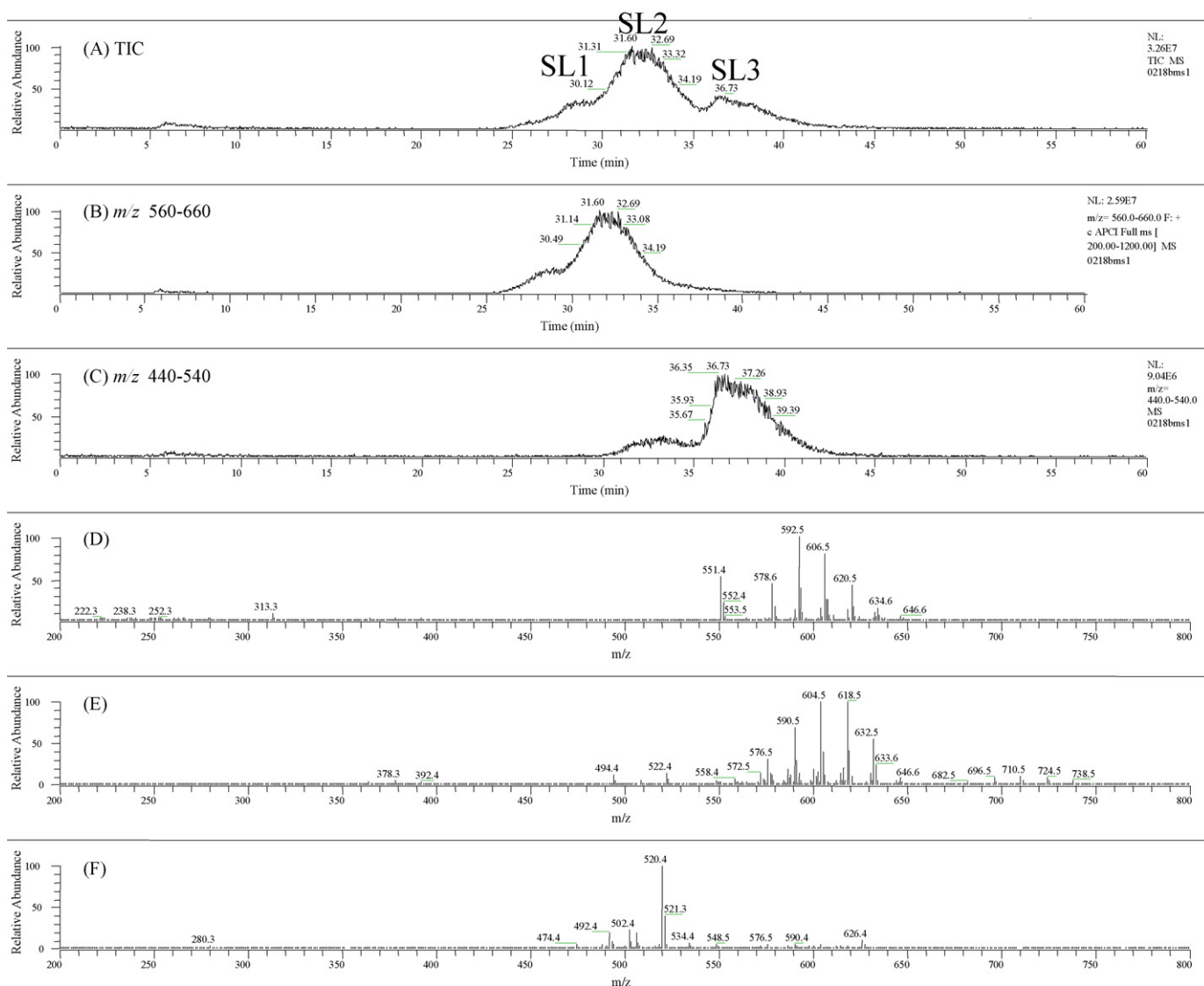


**Fig. 5.** APCI-MS analysis of bovine milk sphingomyelin in parallel with ESI-MS (Fig. 4). (A) TIC; (B)  $m/z$  range 560–660; (C)  $m/z$  range 440–540; (D) average mass spectrum across SL1, 26–29 min; (E) average spectrum across SL2, 29.75–35.5 min; (F) average spectrum across SL3, 35.6–40.

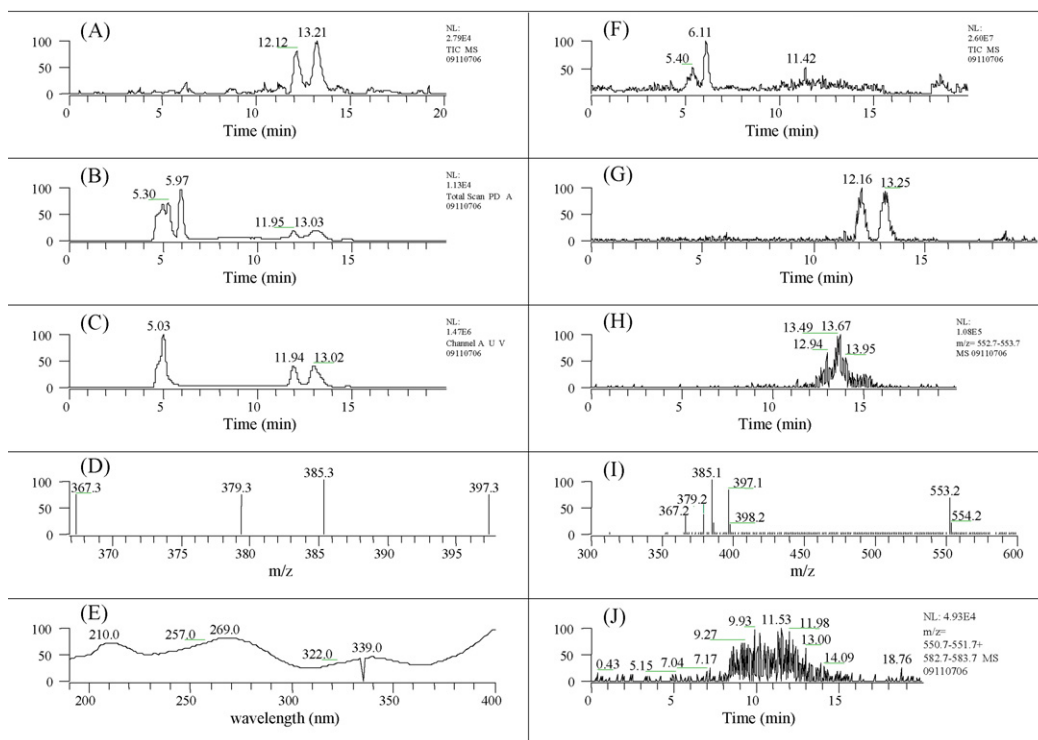
In other words, a mono-unsaturated DSM ‘looks like’ a saturated SM. For this reason, unsaturated DSM species are rarely reported using typical HPLC-ESI-MS techniques. However, since saturated DSM species do not have the same masses as any SM species (saturated DSM are always 2 amu higher), only saturated DSM species are usually reported, if DSM is reported at all. Even saturated DSM is often not reported, since low levels of DSM can be overlooked because they have the same masses as the  $2 \times ^{13}\text{C}$  isotopic peaks of SM. For these reasons, we have shown that the chromatographic resolution of DSM from SM is crucial for proper identification of all DSM and SM molecular species, although complete resolution is not necessary, as Fig. 4 shows.

Fig. 4E shows the long-chain DSM species that eluted in SL1. Bovine milk contains mostly saturated molecular species, such as  $d16:0/23:0$  at  $m/z$  775.6,  $d16:0/24:0$  and  $d18:0/22:0$  at  $m/z$  789.6,  $d18:0/23:0$  at  $m/z$  803.5, and  $d18:0/24:0$  at  $m/z$  817.5, although small abundances of peaks at two mass units lower than the primary peaks are visible. These small peaks represent mono-unsaturated DSM species, such as  $d18:0/22:1$  at  $m/z$  787.6 or  $d18:0/24:1$  at  $m/z$  815.5. Without the prior chromatographic separation, these would be easily confused with SM species  $d18:1/22:0$  and  $d18:1/24:0$ . Bovine milk SM differed from bovine brain and

other sources of SM in the large proportion of odd-chain SM and DSM species, evidenced by peaks such as  $d16:0/23:0$  at  $m/z$  775.6 or  $d18:0/23:0$  at  $m/z$  803.5.

Negative-ion ESI-MS of SM and DSM gave exclusively formate adducts, presumably formed by coordination of the formate moiety with the positive quaternary amine, leaving a net negative on the phosphate group. Fig. 4F, H and J, therefore, exhibit ions at  $[M+45]^-$ , which are 44 mass units higher than all of the  $[M+H]^+$  ions (assuming SM and DSM are zwitterionic, and form an  $[M+H]^+$  when a proton is added to the phosphate, leaving a net positive on the quaternary amine) in Fig. 4E, G, and I. The positive- and negative-ion ESI-MS spectra provided mutually confirmatory pieces of data that readily allowed the molecular weights of the numerous molecular species of SM and DSM to be identified.

Since ESI-MS/MS of the choline-containing precursors yielded only the  $m/z$  184.2 ion, we used APCI-MS, Fig. 5, to provide ceramide-like fragments of the DSM and SM species. It is easily seen that every peak in Fig. 5D–F corresponds to the neutral loss of a zwitterionic phosphocholine head group,  $-\text{PO}_4^- - \text{CH}_2\text{CH}_2\text{N}^+(\text{CH}_3)_3$ , for a difference of 183 amu from each peak in Fig. 4E, G and I, respectively. These fragments are not produced by ESI-MS/MS, so APCI-MS represents a valuable complementary technique to pro-



**Fig. 6.** Dual parallel mass spectrometry using selected ion monitoring (SIM) APCI-MS for quantification, and qualitative full-scan APCI-MS. (A) SIM APCI-MS TIC; (B) UV total scan; (C) UV at 265 nm; (D) SIM mass spectrum 11.68–14 min; (E) UV spectrum across vitamin D<sub>3</sub> peak 12.62–13.73 min; (F) APCI-MS TIC; (G) EIC for vitamin D<sub>2</sub> and D<sub>3</sub> [M+H]<sup>+</sup> and [M+H–H<sub>2</sub>O]<sup>+</sup> ions; (H) EIC for *m/z* 553.2; (I) APCI-MS mass spectrum from 11.68 to 14 min; (J) EIC of *m/z* 551.2 and 583.2.

vide structural information on sphingolipid species. Based on the combination of ceramide-like fragments from APCI-MS and protonated molecules and formate adducts by ESI-MS we identified a large number of molecular species that were then subjected to further analysis using APCI-MS/MS, not in parallel, which is not presented here [25]. Dual parallel mass spectrometry data such as that in Figs. 4 and 5 allowed us to prove conclusively that dihydrosphingomyelin is a component of cow's milk, and is therefore a dietary sphingolipid.

### 3.3. LC1/MS2 of vitamin D<sub>3</sub> in orange juice

Selected ion monitoring APCI-MS is useful for vitamin D analysis in foods [26,29,30], because APCI-MS readily produces a protonated molecule, [M+H]<sup>+</sup>, and dehydrated protonated molecule, [M+H–H<sub>2</sub>O]<sup>+</sup>, from underivatized vitamin D<sub>3</sub> and from vitamin D<sub>2</sub>, which is often used as the internal standard for analysis. Several authors have, however, mentioned that there are interfering species that overlap with vitamin D<sub>3</sub> and/or vitamin D<sub>2</sub> that can interfere with quantification of the analyte when using SIM APCI-MS [26,29,30]. A typical example is demonstrated by our initial analysis of orange juice samples using a Vydac column for the chromatographic separation in AOAC 2002.05 [31]. Fig. 6 shows the SIM APCI-MS and UV data in the left panel. Fig. 6A shows the SIM ions, [M+H]<sup>+</sup> and [M+H–H<sub>2</sub>O]<sup>+</sup>, for vitamin D<sub>2</sub> and D<sub>3</sub>, and gives no indication that there is any overlapping or interfering species. However, the total scan UV chromatogram in Fig. 6B shows a broadened peak that indicates a problem with overlapping chromatographic peaks at ~13 min, where vitamin D<sub>3</sub> eluted. Fig. 6C is the chromatogram of the single channel UV detection at 265 nm, which shows a slightly broadened peak, but not a distinct interferent. The SIM ions in Fig. 6D give no indication of an overlapping species, and would not show any ions unless they were isobaric with the protonated molecule or dehydrated protonated molecule. Fig. 6E, however, shows a full-scan UV spectrum that is distinctly differ-

ent from the normal spectrum for vitamin D, which should have a maximum near 265 nm, and no substantial absorbance at longer wavelength. Thus, only the total-scan UV chromatogram and the UV full spectrum provide a good indication of chromatographically unresolved peaks at the retention time of vitamin D<sub>3</sub>. Obviously, quantification based on UV detection would give erroneous results due to overlapping species.

Since we previously reported an overlapping species in the analysis of processed cheese [26], we routinely employ a second mass spectrometer, in parallel for qualitative analysis to supplement the quantification by SIM. While the ions from vitamin D in Fig. 6G provide no indication of overlap, the full-scan APCI-MS spectrum in Fig. 6I shows an abundant peak at *m/z* 553.2 that belongs to an overlapping interferent. The EIC for this mass, Fig. 6H, shows the elution profile for the interferent, and reveals that it coeluted with vitamin D<sub>3</sub> at 13–14 min (MS retention times were ~0.2 min later than UV times, since the MS was after the UV detector in series). Closer examination of the full-scan data allowed other interfering species to be identified, which gave the elution profile shown in Fig. 6J. These data make the value of dual parallel mass spectrometry for simultaneous quantitative and qualitative analysis abundantly clear.

Based on those data, the column was changed to an Inertsil® ODS-2 column, which is thoroughly end-capped and has more than twice the carbon load (18.5% vs. 8%). This provided modified selectivity that moved the interfering species having *m/z* 553.2 to ~17 min. The chromatograms in Fig. 7A–C show sharp, distinct peaks by SIM APCI-MS, total-scan UV and single channel UV at 265 nm detection for a different but similar orange juice sample. The UV spectrum in Fig. 7E is typical of pure vitamin D<sub>3</sub>. A difference can be seen in the ratio of the [M+H]<sup>+</sup> to [M+H–H<sub>2</sub>O]<sup>+</sup> ions, due to the increased amount of methanol, and less acetonitrile, in the solvent system required to elute the analyte and internal standard in the same time window on the end-capped column with higher carbon load. The full-scan spectrum in Fig. 7I shows that the *m/z* 553.2 is no

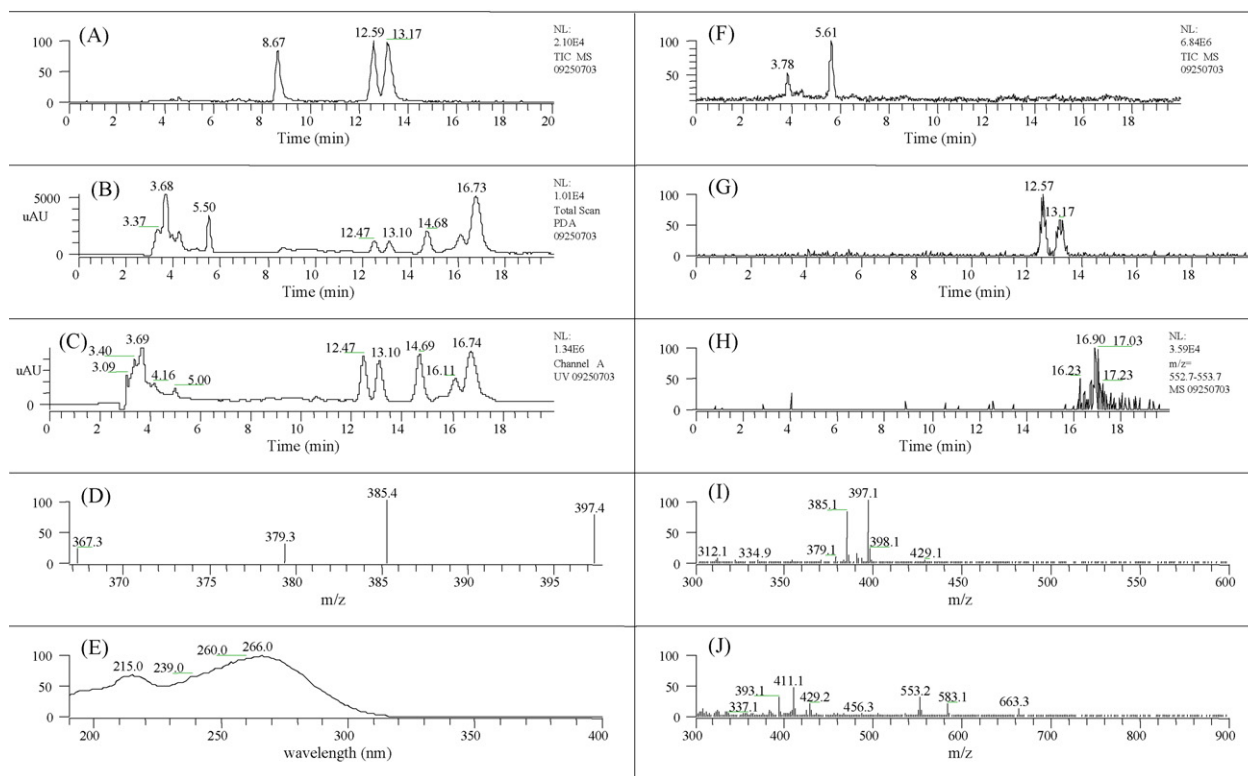


**Fig. 7.** Dual parallel mass spectrometry using SIM APCI-MS for quantification, and qualitative full-scan APCI-MS. (A) SIM APCI-MS TIC; (B) UV total scan; (C) UV at 265 nm; (D) SIM mass spectrum 12.3–13.6 min; (E) UV spectrum across vitamin D<sub>3</sub> peak 13–13.2 min; (F) APCI-MS TIC; (G) EIC for vitamin D<sub>2</sub> and D<sub>3</sub> ions; (H) EIC for *m/z* 553.2; (I) APCI-MS mass spectrum from 12.3 to 13.6 min; (J) average mass spectrum from 14.4 to 17.4 min.

longer present at the retention time of vitamin D<sub>3</sub>, and Fig. 7H shows its retention time, ~17 min, on the new column. The mass spectrum in Fig. 7J is an average mass spectrum across the time range 14.4–17.4 min, and provides qualitative information about the later eluting peaks seen in Fig. 7B and C. Thus, the dual parallel mass spectrometry arrangement provided valuable confirmation that the vitamin D<sub>2</sub> and vitamin D<sub>3</sub> peaks were resolved from interfering species, which allowed them to be quantified based on UV detection at 265 nm, as well as by SIM APCI-MS, with confidence. The sample shown in Fig. 7 contained  $14.75 \pm 0.14$  ng/g sample, or  $59.00 \pm 0.58$  IU/100 g ( $1 \mu\text{g} = 40$  IU) determined from UV data (Fig. 7C) or  $14.15 \pm 0.30$  ng/g sample, or  $56.6 \pm 1.2$  IU/100 g by SIM APCI-MS (Fig. 7A), which translates to 140 IU per 8 oz. glass of juice, by UV detection.

### 3.4. LC2/MS2 of bovine brain total lipid extract

Most commonly, either polar lipids (i.e. phospholipids) or neutral lipids (i.e. triacylglycerols) are separated using normal-phase HPLC or reversed-phase HPLC, to the exclusion of the other class. In the field of 'lipidomics', however, information is sought for all molecular species from all classes of lipids, both polar and non-polar [16,17,32,33]. Therefore, we have implemented a separation technique that employs two liquid chromatography systems connected via an electronic switching valve that is used for that analysis of all polar and non-polar lipids in one analysis, referred to as an LC2/MS2 approach. This is in contrast to other multi-dimensional techniques that typically apply two dimensions of chromatography to the same class of molecules, so that each molecule has a retention time in two dimensions. Conventional two-dimensional liquid chromatography separations for food and lipid analysis have been

reported and reviewed extensively by Dugo et al. in recent years [13,34–36].

Fig. 8 shows the normal-phase separation of polar lipids, including phospholipids and glycosphingolipids detected using ESI-MS and MS/MS. Neutral lipids were not substantially retained on this column and came off the column as an early-eluting bolus, which was diverted through the electronically controlled valve on the front of the ion trap mass spectrometer. The neutral lipids were diverted to a RP-HPLC system, and separated as shown in Fig. 9, also using ESI-MS/MS for detection.

Fig. 8A is the TIC that displays the alternating positive ion and negative ion, as well as MS and MS/MS scans. The positive-ion full-scan filtered EIC is seen in Fig. 8B, while the corresponding negative-ion full-scan EIC is in Fig. 8C. Comparison of the chromatograms highlights the responses of the different classes under opposite ionization conditions: phosphatidylcholine (PC) gave more signal by positive than by negative ionization, whereas glycosphingolipids responded better by negative ionization. All three classes of galactosphingolipids that were observed (galactoceramide, hydroxygalactoceramide and sulfatogalactoceramide, assumed to be galacto-based on the SphinGOMap at [www.SphinGOMap.com](http://www.SphinGOMap.com)) produced abundant negative-ion mass spectra (e.g. Fig. 8E), but all three classes produced similar positive-ion spectra (e.g. Fig. 8D), which required great care to differentiate [10] due to the low abundances of protonated molecule ions. On the other hand, the negative-ion mass spectra produced abundant deprotonated molecule ions that allowed the molecular weights of the species to be readily found. The combination of positive- and negative-ion mass spectra was crucial for proper identification of these molecules. Typical averaged ESI-MS/MS spectra in both positive- and negative-ion modes are shown in Fig. 8F and G, respectively.

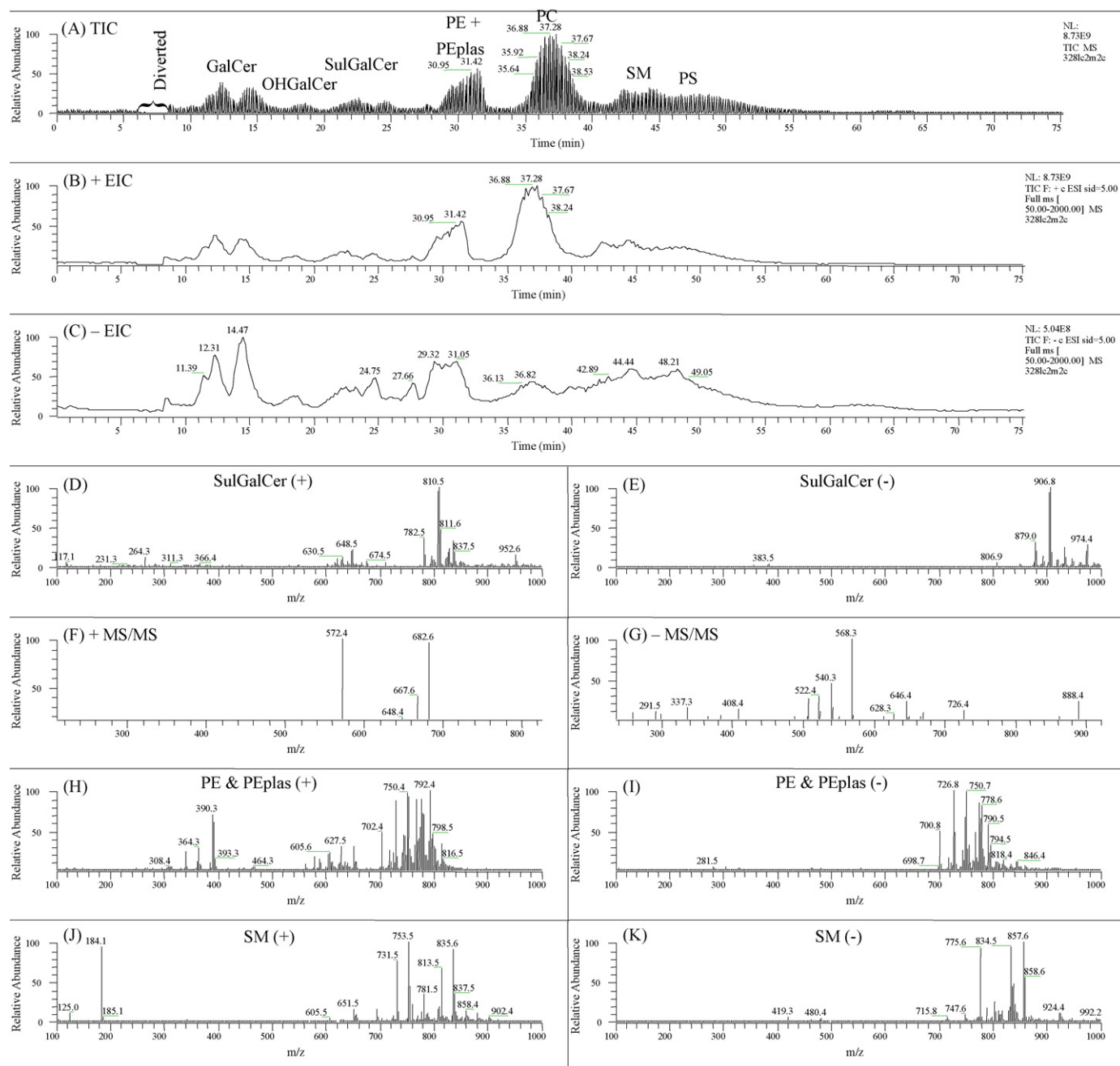


**Fig. 8.** Normal-phase HPLC separation of LC/MS2 analysis using ESI-MS, MS/MS and MS<sup>3</sup>. (A) TIC; (B) TIC filtered to show positive-ion scans; (C) TIC filtered to show negative-ion scans; (D) average positive-ion mass spectrum from 23.5 to 24.9 min; (E) average negative-ion mass spectrum 23.5–24.9 min; (F) positive-ion MS/MS of *m/z* 810.5 at 24.1 min; (G) negative-ion MS/MS of *m/z* 906.8 at 24.0 min; (H) average positive-ion spectrum 29–32 min; (I) average negative-ion spectrum 29–32 min; (J) average positive-ion spectrum 41.75–45.5 min; (K) average negative-ion spectrum 41.75–45.5 min.

Phosphatidylethanolamine species, including their plasmalogen, readily formed protonated molecules and deprotonated molecules in positive- and negative-ion modes, Fig. 8H and I, respectively, and made identification of the molecular masses of the species straightforward. On the other hand, choline-containing sphingolipids formed almost exclusively formate adducts,  $[M+45]^-$ , in negative-ion mode, such as those from sphingomyelin in Fig. 8K. Protonated molecules and sodium adducts were formed from SM in positive mode, as seen in Fig. 8J. PC similarly formed protonated and natriated molecule ions in positive-ion mode, and formate adducts in negative-ion mode. Phosphatidylserine (PS) molecular species formed abundant protonated molecules in positive-ion mode, along with deprotonated

molecules in negative-ion mode, assuming PS in its natural state is zwitterionic, having a negatively charged phosphate group, a neutral carboxylic acid, and a protonated primary amine, as discussed in detail elsewhere [10,11].

Bovine brain total lipid extract showed a smaller amount of neutral lipids than polar ones, as seen in the TIC in Fig. 9A, with the full-scan filtered EIC in Fig. 9B. The neutral lipids were composed mostly of ceramide (Cer) species, DAGs and TAGs, with smaller amounts of cholesterol-related molecules. Fig. 9C shows the average mass spectrum across the large peak at 20.5 min, which was identified as *d*18:1/18:0 Cer. The protonated molecule at *m/z* 566.4, along with the dehydrated protonated molecule at *m/z* 548.4 and sodium adduct at *m/z* 588.4 made identification of this Cer

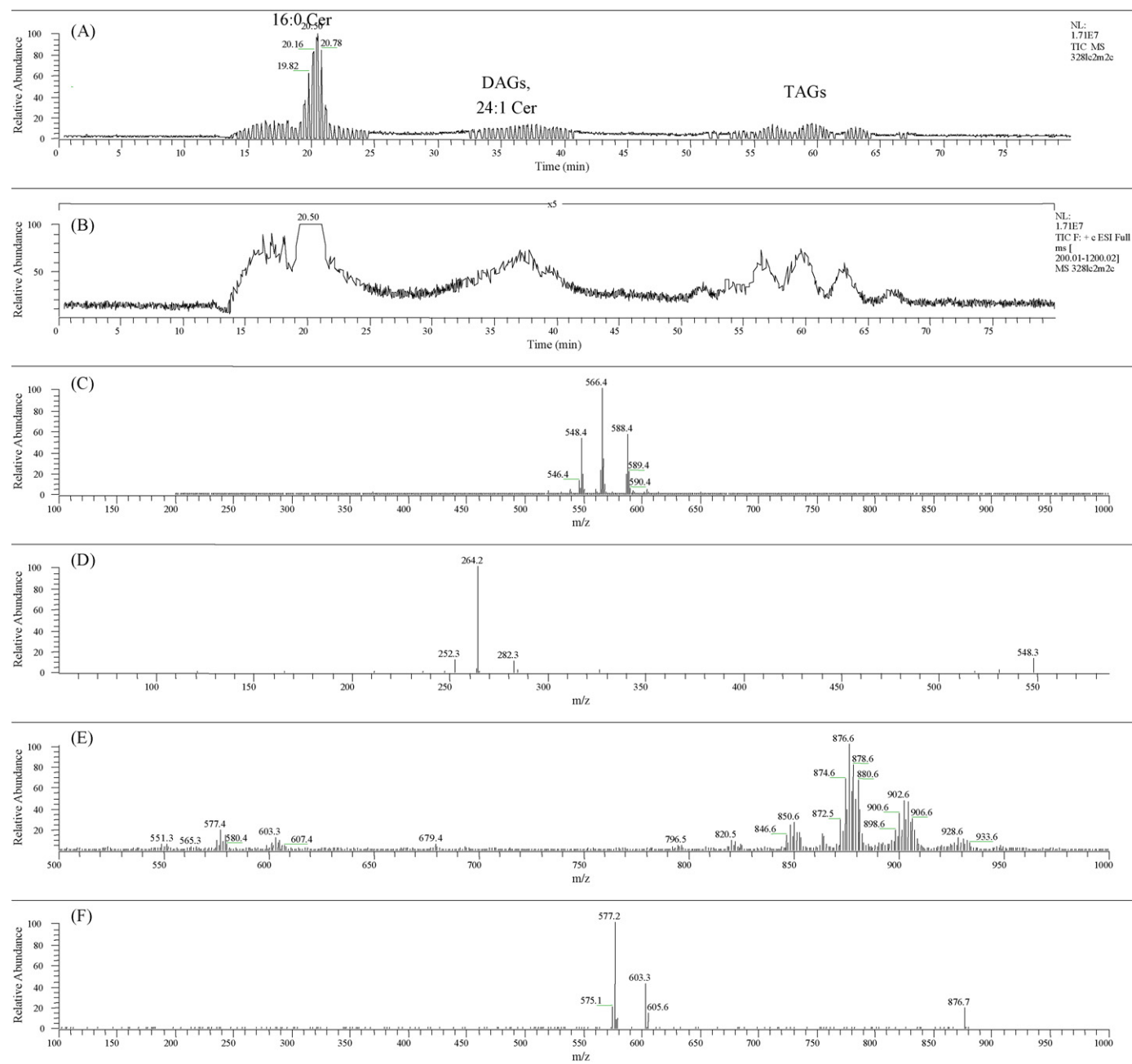


**Fig. 9.** Reversed-phase HPLC separation of diverted (see Fig. 8A) non-polar bolus for LC2/MS2 analysis using ESI-MS and MS/MS. (A) TIC; (B) TIC filtered to show full scans; (C) average mass spectrum 19–21.4 min; (D) average MS/MS spectrum 19.3–21.4 min; (E) average mass spectrum 50–70 min; (F) average MS/MS spectrum 50–70 min.

straightforward. The identity was confirmed by the long-chain base fragment,  $[\text{LCB}]^+$ , at  $m/z$  264.2 and dehydrated long-chain base fragment,  $[\text{LCB}-\text{H}_2\text{O}]^+$ , at  $m/z$  252.3 in the ESI-MS/MS spectrum of the  $m/z$  566.4 precursor, shown in Fig. 9D.

For illustration of identification of TAGs, an average mass spectrum over all TAGs from 50 to 70 min is shown in Fig. 9E. Since ESI was used, the ammonium adducts were formed, as described in Section 3.1. A variety of molecular species can be identified in Fig. 9E, with the largest cluster being those having ACN 52 ( $2 \times \text{C}18:n+1 \times \text{C}16$ ), and the most abundant TAG being OOP. The average ESI-MS/MS mass spectrum across the same time range showed the corresponding  $[\text{DAG}]^+$  fragments. As expected, the largest  $[\text{DAG}]^+$  was  $[\text{OP}]^+$  at  $m/z$  577.2, with  $[\text{OO}]^+$ ,  $[\text{LP}]^+$ ,  $[\text{OS}]^+$ , and others readily apparent. Full discussion of the LC2/MS2 of bovine brain [10,37] and of sand bream file [11,37] has been presented elsewhere. The data shown here exemplify the value of employ-

ing two separation techniques with different modes of retention used in parallel for molecules differing substantially in polarity that are part of a total lipid extract. Combined with mass spectrometric techniques using positive and negative polarities, and with MS/MS, a great number of individual molecular species from a wide range of lipid classes can be identified for a complete lipidomic analysis.

#### 4. Conclusion

Examples here have shown the benefits of APCI-MS and -MS/MS combined with ESI-MS, -MS/MS, and -MS<sup>3</sup> of TAGs, positive and negative ESI-MS combined with APCI-MS for sphingolipids, and SIM APCI-MS for quantitative analysis combined with full-scan APCI-MS for qualitative analysis. When used in simultaneously in parallel, these techniques produce a wealth of data that provide mutually confirmatory ions and fragments that increase the certainty of

molecular identifications. By obtaining such data simultaneously, the retention times on different machines are essentially identical, which eliminates the inevitable uncertainty that is inherent in replicate chromatographic runs (retention times by LC1/MS2 are identical if equal lengths of tubing are used, or have a constant offset if different lengths are employed). Even small changes in retention times can lead to ambiguity when analyzing large numbers of molecules in a complex lipid mixture. The dual parallel mass spectrometer arrangement eliminates this source of uncertainty. It should be noted that it is beneficial to synchronize the clocks on multiple workstations to make it easier to identify parallel runs, although this does not affect retention times.

Given the large variety of combinations of ionization types,  $MS^n$ , and scan modes (e.g. SIM, MRM, full scan, neutral loss, etc.), a dual parallel arrangement allows more types of data to be acquired in a shorter amount of time than conducting each desired experiment independently. This saves time, resources (solvents, etc.), and can be especially valuable in cases of limited sample amounts. Given the affordability of high quality used instruments, cost is no longer a prohibition against the use of dual parallel mass spectrometers. Or, as labs upgrade to newer, faster, more sensitive instruments, there is benefit in keeping older instruments in service as auxiliary detectors to provide confirmatory or complementary data.

The benefits of the LC2/MS2 column-switching approach are obvious. It allows all polar and non-polar lipids to be analyzed in one run for a total lipid analysis. This has numerous potential applications in lipidomics and elsewhere. For instance, the fact that ceramide is the product of *sphingomyelinase* activity on sphingomyelin in cellular signaling pathways, and that ceramide was separated on the reversed-phase system while sphingomyelin eluted on the normal-phase system, leads to the possibility of monitoring the individual molecular species of the precursor and product in a cellular system simultaneously using an LC2/MS2 approach. Of course the dual parallel mass spectrometry and LC2/MS2 approaches are not mutually exclusive. Dual parallel mass spectrometry could be used in either or both of the separations used for the total lipid analysis, so LC2/MS3 or LC2/MS4 experiments are possible. The only limitations seem to be the imagination and expertise of the operator, and the time necessary to process the plethora of data that results from such LCx/MSy experiments.

### Acknowledgements

Portions of this work were supported by the USDA Agricultural Research Service. The work and assistance of William E. Neff and Richard H. Perry is gratefully acknowledged.

### References

- [1] W.C. Byrdwell, *INFORM Int. News Fats Oils Relat. Mater.* 9 (1998) 986.
- [2] W.C. Byrdwell, *Lipids* 36 (2001) 327.
- [3] T. Rezanka, K. Sigler, *Curr. Anal. Chem.* 3 (2007) 252.
- [4] W.C. Byrdwell, in: R.O. Adlof (Ed.), *Advances in Lipid Methodology—Five*, P.J. Barnes, Bridgewater, UK, 2003, p. 171.
- [5] W.C. Byrdwell, in: W.C. Byrdwell (Ed.), *Modern Method for Lipid Analysis by Liquid Chromatography/Mass Spectrometry and Related Techniques*, AOCS Press, Champaign, IL, 2005, p. 298.
- [6] Lipid Library, In: William W. Christie (Ed.), *American Oil Chemists' Society*. [http://www.lipidlibrary.co.uk/lit\\_surv/ms\\_ms/apci\\_ms.htm](http://www.lipidlibrary.co.uk/lit_surv/ms_ms/apci_ms.htm) (accessed 11-9-2009).
- [7] Lipid Library, In: William W. Christie (Ed.), *American Oil Chemists' Society*. [http://www.lipidlibrary.co.uk/lit\\_surv/ms\\_ms/electms2.htm](http://www.lipidlibrary.co.uk/lit_surv/ms_ms/electms2.htm) (accessed 11-9-2009).
- [8] J. Folch, M. Lees, G. Sloane Stanley, *J. Biol. Chem.* 226 (1957) 497.
- [9] E.G. Bligh, W.J. Dyer, *Can. J. Biochem. Phys.* 37 (1959) 911.
- [10] W.C. Byrdwell, *J. Liq. Chromatogr. Relat. Technol.* 26 (2003) 3147.
- [11] W.C. Byrdwell, *Front. Biosci.* 13 (2008) 100.
- [12] P. Dugo, T. Kumm, B. Chiofalo, A. Cotroneo, L. Mondello, *J. Sep. Sci.* 29 (2006) 1146.
- [13] P. Dugo, T. Kumm, F. Cacciola, G. Dugo, L. Mondello, *J. Liq. Chromatogr. Relat. Technol.* 31 (2008) 1758.
- [14] E.J.C. van der Klift, G. Vivo-Truyols, F.W. Claassen, F.L. van Holthoon, T.A. van Beek, *J. Chromatogr. A* 1178 (2008) 43.
- [15] I. Francois, P. Sandra, *J. Chromatogr. A* 1216 (2009) 4005.
- [16] M.R. Wenk, *Nat. Rev. Drug Discov.* 4 (2005) 594.
- [17] C. Wolf, P.J. Quinn, *Prog. Lipid Res.* 47 (2008) 15.
- [18] N. Zehethofer, D.M. Pinto, *Anal. Chim. Acta* 627 (2008) 62.
- [19] X. Han, R.W. Gross, *Expert Rev. Proteom.* 2 (2005) 253.
- [20] X. Han, R.W. Gross, *Mass Spectrom. Rev.* 24 (2005) 367.
- [21] E. Fahy, S. Subramaniam, R.C. Murphy, M. Nishijima, C.R. Raetz, T. Shimizu, F. Spener, G. Van Meer, M.J. Wakelam, E.A. Dennis, *J. Lipid Res.* 50 (Suppl.) (2009).
- [22] P.R. Pehrsson, D.B. Haytowitz, J.M. Holden, C.R. Perry, D.G. Becker, *J. Food Compos. Anal.* 13 (2000) 379.
- [23] AOAC Official Method 992.26, *Official Methods of Analysis of AOAC International*, AOAC International, Gaithersburg, MD, 1999, p. 50.1.05.
- [24] W. Byrdwell, W.E. Neff, *Rapid Commun. Mass Spectrom.* 16 (2002) 300.
- [25] W. Byrdwell, R.H. Perry, *J. Chromatogr. A* 1146 (2007) 164.
- [26] W.C. Byrdwell, *J. Agric. Food Chem.* 57 (2009) 2135.
- [27] W.C. Byrdwell, E.A. Emken, *Lipids* 30 (1995) 173.
- [28] W.C. Byrdwell, R.H. Perry, *J. Chromatogr. A* 1133 (2006) 149.
- [29] G. Dimartino, *J. AOAC Int.* 90 (2007) 1340.
- [30] O. Heudi, M.J. Trisconi, C.J. Blake, *J. Chromatogr. A* 1022 (2004) 115.
- [31] AOAC Official Method 2002.05, in: W. Horwitz, G. Latimer Jr. (Eds.), *Official Methods of Analysis of AOAC International*, AOAC International, Gaithersburg, MD, 2007, p. 45.1.22A.
- [32] N. Navas-Iglesias, A. Carrasco-Pancorbo, L. Cuadros-Rodriguez, *TrAC Trends Anal. Chem.* 28 (2009) 393.
- [33] L.D. Roberts, G. McCombie, C.M. Titman, J.L. Griffin, *J. Chromatogr. B: Anal. Technol. Biomed. Life Sci.* 871 (2008) 174.
- [34] P. Dugo, F. Cacciola, T. Kumm, G. Dugo, L. Mondello, *J. Chromatogr. A* 1184 (2008) 353.
- [35] P.Q. Tranchida, P. Dugo, G. Dugo, L. Mondello, *J. Chromatogr. A* 1054 (2004) 3.
- [36] P.Q. Tranchida, P. Donato, G. Dugo, L. Mondello, P. Dugo, *TrAC Trends Anal. Chem.* 26 (2007) 191.
- [37] W.C. Byrdwell, in: W.C. Byrdwell (Ed.), *Modern Method for Lipid Analysis by Liquid Chromatography/Mass Spectrometry and Related Techniques*, AOCS Press, Champaign, IL, 2005, p. 510.